SYNCHRONISATION ON ASTRONOMICAL FORCING

MICHEL CRUCIFIX, BERNARD DE SAEDELEER,
GUILLAUME LENOIR, DAVID GARCIA - ALVAREZ,
Georges Lemaitre Centre for Earth and Climate Resarch, Earth and Life Institute,
Université catholique de Lauvoin, 2 chemin du Cyclotron,
BE-1348 Louvain-la-Neuve, Belgium
itop@uclouvain.be

submitted to International of Bifurcation and Chaos on 30.09.2010

Abstract

There is wide evidence and acceptation that ice age cycles are *paced* by changes in the seasonal and spatial distributions of insolation, induced by variations in the astronomical elements of planet Earth. However, the usual concept of phase-locking is reserved for periodic forcings. Here, we introduce the cardinality of the pullback attractor as a useful measure of synchronisation in the context of a quasi-periodic forcing, such as the astronomical forcing. The concept is illustrated with a small palaeoclimate model akin of the celebrated Van der Pol oscillator. At low forcing amplitude the system may lock on the individual components of the astronomical forcing in a way that is similar to phase-locking on periodic forcing, but as the amplitude is increased the combined effects of precession and obliquity restrict the number of possible climate histories. We describe a phenomenon similar to the 'phase-slip' encountered in periodic-forced systems subject to additive fluctuations and comment on its relevance and consequences at palaeoclimate time scales. *Keywords:* Climate, Milankovitch, synchronisation, AUTO, Lyapunov exponent, pullback attractor.

1 Introduction

The present contribution focuses on the slow variations of climate over the last million years. This includes the phenomenon of ice ages, that is, the repeated growth and decay of ice sheets in the Northern

Hemisphere of a total mass as big as modern Antarctica's. The four most recent cycles cover the last 400,000 years and have distinctive saw-tooth dynamics, with slow growths of ice followed by abrupt 'deglaciations'. The previous cycles are more symmetric but conserve the average periodicity of 100,000 years (e.g. *Lisiecki and Raymo*, 2005). The numerous natural archives of climate sampled since the 1950's have made it clear that ice ages involve all the components of the climate system (e.g. *Petit et al.*, 1999).

Modelling and understanding ice ages is a vast and not well-defined problem. We believe that a good model should be consistent with as many climate records as possible, it should be compatible with constraints deduced from experiments with complex numerical models of the the climate system, and it should be mathematically tractable. Such a model may naturally be expressed as a stochastic dynamical system in which account is made of unresolved processes and uncertainties.

Catherine Nicolis was among the first ones the study ice ages using theories of deterministic and stochastic dynamical systems. *Nicolis and Nicolis* (1984) and *Nicolis and Nicolis* (1986) questionned whether palaeoclimate time series contain an underlying low-dimensional structure. Application and analysis of the *Grassberger and Procaccia* (1983) algorithm to a deep-sea record lead them to suggest a positive answer to that question. Unfortunately, the attractor dimension estimates provided by the algorithm later appeared to lack robustness due to short time-series length, dating uncertainties and non-stationarity effects *Grassberger* (1986); *Mudelsee and Stattegger* (1994). Two other articles *Nicolis and Nicolis* (1981); *Nicolis* (1982) address more specifically the distribution of climatic states subject to the combined effects of a *climatic potential* and additive fluctuations. The work relies on the resolution of Fokker-Plank equations and lent theoretical support to the notion of *stochastic resonance* then just introduced by *Benzi et al.* (1982). Specifically, it was proposed that the transitions between glacial and interglacial states are noise-assisted amplifications of the slow and slight variations in total incoming solar radiation related to changes in Earth's orbital eccentricity. Although our understanding of palaeoclimate dynamics has considerably evolved since then, these contributions have successfully seeded the fertile field of palaeoclimate dynamics theory. It justified the development and application of more advanced time-series analysis methods (e.g.: singular spectrum analysis *Vautard and Ghil* (1989)), as well as the development of other dynamical models of palaeclimates, notably by *Ghil and Le Treut* (1981), *Saltzman et al.* (1984) and many others (further references in the sequel). Palaeoclimate dynamics theory is today an active research field.

Here we concentrate on the influence of the astronomical forcing of Earth's climate. This forcing is induced by the slow variations in the spatial and seasonal distributions of incoming solar radiation (insolation) at the top of the atmosphere, associated with the slow variations of the Earth's eccentricity (e),

true solar longitude of the perihelion measured with respect to the moving vernal equinox (ϖ), and Earth obliquity (ε). These quantities are now accurately known over several tens of millions of years *Laskar et al.* (2004), but analytical approximations of e, $e\sin\varpi$ and ε valid back to one million years have been known since *Berger* (1978). They take the form of d'Alembert series ($\sum a_i \sin[\omega_i t + \phi_i]$). Most insolation quantities relevant for understanding ice ages are well approximated as a linear combination of $e\sin\varpi$, $e\cos\varpi$ and ε. Thanks to *Berger*'s formulæ, estimating the spectrum decomposition of any insolation measure reduces to a simple linear regression problem of insolation on astronomical parameters.

Figure 1 shows a spectrum decomposition of insolation at 65°N latitude on the day of the summer solstice. This quantity is commonly related to the Milankovitch hypothesis because it is thought to be a measure of how much ice may melt over summer. The spectrum is somewhat complex. Precession is dominated by two harmonics around 19 and 23 ka (1ka $= 1,000$ years) and obliquity is dominated by a harmonic with a period of 41 ka but it bears periods as long as 1,200 ka.

There is ample evidence that the astronomical forcing influences the climate system. The phrase 'pacemaker of ice ages' was coined in a seminal paper *Hays et al.* (1976) to express the idea that the timing of ice ages is controlled by the astronomical forcing, while the ice age cycle itself is shaped by internal system dynamics. The paradigm has prevailed since then and is it still supported by the most recent analyses of palaeoclimate records *Lisiecki and Raymo* (2007); *Huybers* (2007).

The notion of 'pacemaker' naturally evokes synchronisation and 'phase locking' in dynamical system theory. However, the very concept of phase locking cannot be applied straightforwardly because it is not possible to define an instantaneous phase of the astronomical forcing because it is dominated by several distinct harmonics. We will therefore focus on another concept: the cardinality of the pullback attractor.

The article is structured as follows. Section 2 introduces a slightly modified version of the Van der Pol oscillator as a suitable model for the purpose of studying synchronisation of ice ages. In Section 3 we briefly review the well-known synchronisation properties of this oscillator on a periodic forcing, and highlights the correspondence between the bifurcation diagram and numerical estimates of the cardinality of the pullback attractor. We then introduce the astronomical forcing. Section 4 tentatively explores the role of additive fluctuations to the system, by reference to the greatest Lyapunov exponent and geometry of basins of attractions. To be clear, all the treatment below is deterministic, except for Figure 7.

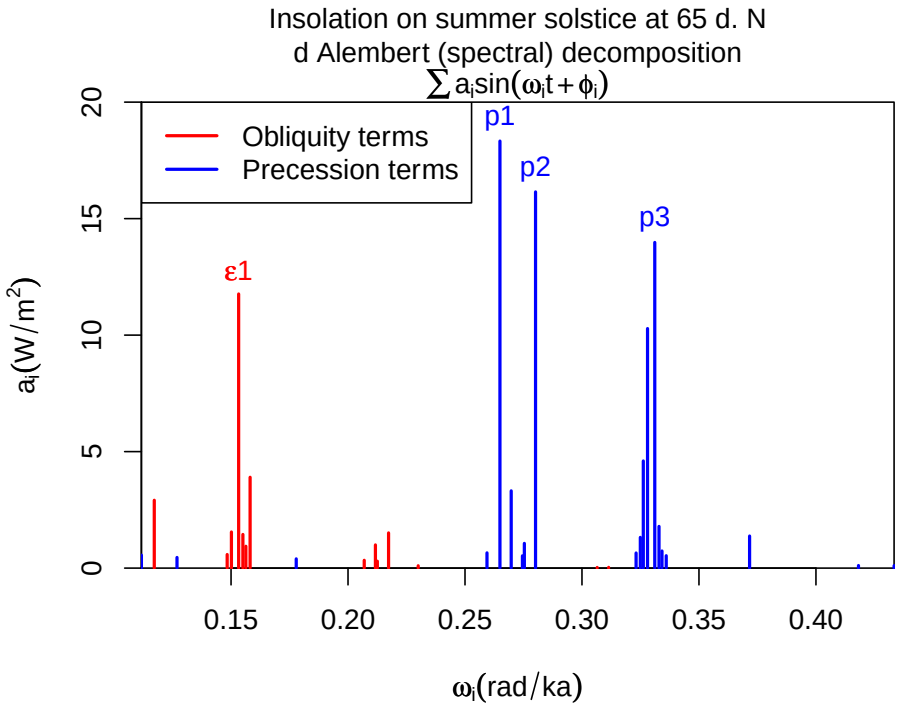

Figure 1: Visualisation of the d'Alembert decomposition of incoming solar insolation (insolation) at 65°N on the day of summer solstice. The d'Alembert decomposition is a sum of the form $\sum a_i \sin(\omega_i + \phi_i)$. The decomposition is obtained first by calculating insolation according to *Berger* (1978), and then regress on the climatic astronomical parameters $e\sin\varpi$, $e\cos\varpi$ and ε, and using the d'Alembert decompositions of these three quantities available as tables in *Berger* (1978). This insolation is the forcing used to construct Figures 2, 4, 6 and 7.

2 The Van der Pol oscillator as a model of ice ages

The hypothesis at the basis of *Milankovitch*'s works [1941] is that changes in total amount of continental ice (say: x) are driven by summer insolation (say: $F(t)$). One straightforward expression of this hypothesis in the form of a dynamical system would be $\dot{x} = -\phi'(x) - \gamma F(t)$, where $\phi'(x)$ is the derivative of a climatic potential and γ a forcing 'efficacy'. However, models of this form fail in practice to correctly capture the rapid deglaciation phenomenon. We therefore propose a model resembling the Van der Pol oscillator:

$$\tau\dot{x} = -(y + \beta + \gamma F(t)) \tag{1a}$$

$$\tau\dot{y} = -\alpha(\psi'(y) - x), \quad \psi'(y) = y^3/3 - y \tag{1b}$$

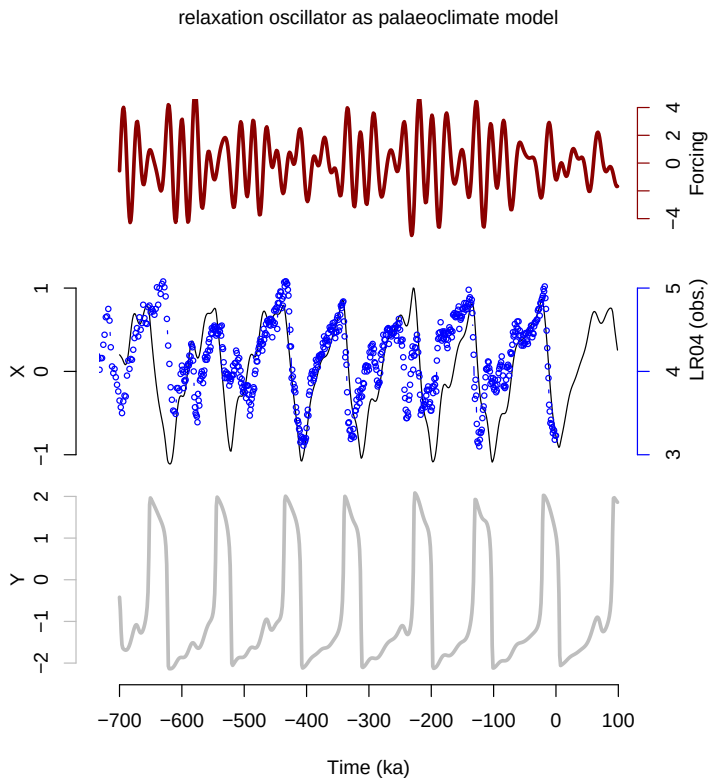

Figure 2: Forcing (corresponding to the decomposition shown on Figure 1, scaled as explained in section 3.2), X and Y trajectories obtained using system (1) with $\alpha = 30$, $\beta = 0.75$, $\gamma = 0.4$ and $\tau = 36$ ka. With these parameters $\omega_{\varepsilon 1} = 2.5\omega_N$, were $\omega_{\varepsilon 1}$ is the angular velocity associated with the dominant harmonic of obliquity and ω_N is the angular velocity associated with the unforced system's periodic orbit. Blue dots are an authoritative natural archive thought to mainly represent ice volume inferred from the oxygen isotopic ratio of foraminifera sampled in the deep seas of the different oceans, and compiled by *Lisiecki and Raymo* (2005). Time= 0 corresponds conventionally to the year 1950 AC.

Its physical interpretation is as follows: x (ice volume) integrates the external forcing over time but with a drift $y + \beta$; y is a faster variable (assuming $\alpha \gg 1$), the dynamics of which is controlled by a two-well potential $\psi(y)$. For example, there are arguments that the dynamics of the Atlantic ocean circulation may respond to an equation of the form of (1b) *Rahmstorf et al.* (2005); *Dijkstra and Weijer* (2005). *Saltzman et al.* (1984); *Tziperman and Gildor* (2003); *Paillard and Parrenin* (2004); *Tziperman et al.* (2006) provide further interpretation and discussion of what the fast variable could be in this context. Parameter τ sets the time scale. The coupled system (1) has one stable solution for $|\beta| > 1$ and a stable periodic orbit for $|\beta| < 1$. The ratio of times spent near the two branches of the slow manifold $\psi'(y) = x$ is

then set by β. In the sequel we note T_N the time of the periodic orbit, and $\omega_N := 2\pi/T_N$ the corresponding mean angular velocity.

We acknowledge that the potential function associated to x is flat and hence unphysical, but we adopted this form because it is very close to the well studied Van der Pol oscillator, and a good agreement with ice volume proxies was easily found for well chosen values of α, β, γ and τ (Figure 2). We note, though, that small changes in parameters or additive fluctuations can easily shift the timing of terminations for reasons that will be clarified in the sequel.

3 Synchronisation of the palaeoclimate model

3.1 Periodic forcing

The case of periodic forcing [$F(t) = \sin(\omega t)$] with $\beta = 0$ was extensively studied, analytically assuming some approximations (*Guckenheimer and Holmes*, 1983, pp. 70-75), and using numerical algorithms for pseudo-arc length continuation *Mettin et al.* (1993). The classical approach consists in embedding the forcing as a third variable, and then explore the parameter space (ω, γ). The case $\alpha = 11.1$, $\beta = 0.25$ is succinctly analysed here using the AUTO continuation software *Doedel and Oldeman* (2009) (Figure 3).

The pattern is reminiscent of *Arnol'd tongues*. Periodic solutions are found in tongues (shaded) which originate at $\omega = m/n \cdot \omega_N$. In practice they are identified by the fact that the Poincaré sections along a given phase of the forcing have a countable set of m stable fixed points impressed in n rotations in the (x, y) plane. Tongues boundaries are fold bifurcations of these solutions. Outside the tongues there are different possibilities: between the tongues at low forcing amplitude the system lives on an invariant torus: trajectories are quasi periodic and Poincaré sections are closed curves; at higher forcing amplitude and in particular above the 1:1 tongue the system enters a *suppression regime* via a fold or a Neimark-Sacker bifurcation (*Balanov et al.*, 2009, pp. 56-62). Trajectories have then the same period as the forcing. Chaotic solutions appear at yet higher forcing amplitude *Mettin et al.* (1993) but this case is beyond our focus.

Regions where tongues overlap are notoriously complex and several stable synchronised solutions may co-exist. The asymmetry introduced here with the parameter β causes some additional complications. In particular there are two stable 3:2 synchronisation regimes (shaded in red and green on Figure 3). Furthermore, at least one of the two 3:2 tongues as well as the 2:1 tongue can be continued for ω/ω_N

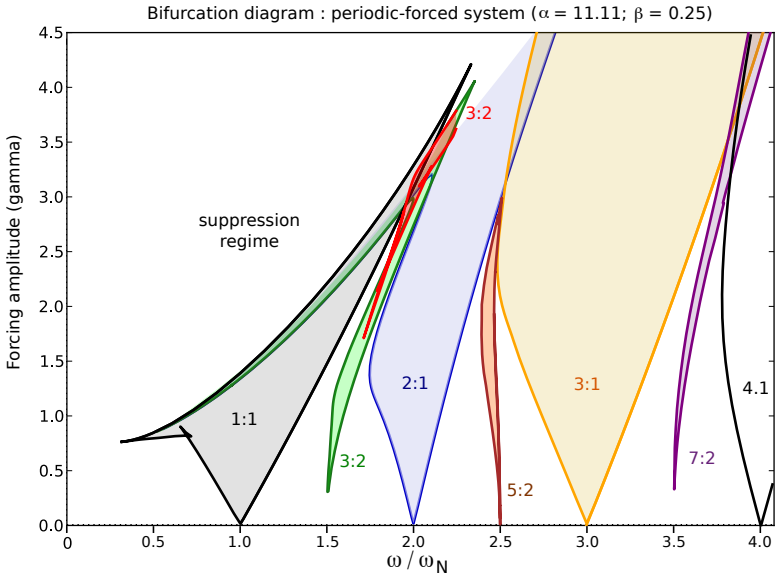

Figure 3: Partial bifuraction diagram of the forced system (1) with $F(t) = \gamma\sin(\omega t)$ obtained as follows: synchronised solutions are first found empirically. They are then continued using AUTO-07P at fixed γ until limit points, and the latter are continued in the γ, ω space. The graphics were produced using the PyPLAUT utility made available with AUTO-07P, but shading and annotations were made manually. In particular, solutions within the 3:2 and 2:2 tongues were found to continue to low values of ω_N in the form of very weakly stable 3:3 and 2:2 periodic solutions, but the tongues could not be closed and the shading is tentative. Fixed parameters are $\alpha = 11.11$ and $\beta = 0.25$ (the graph as presented here is invariant to choices of τ because we are interested in ω/ω_N).

ratios approaching 1. The 3:2 and 2:1 periodic solutions are then continuously transformed into what we call '2:2' or '3:3' solutions, in the sense that the oscillator revolves 2 or 3 times around the origin within 2 or 3 forcing periods. These solutions are very weakly stable and the tongues could not be closed with AUTO. (*Schilder and Peckham* (2007) proposed an algorithm for identification of higher-order tongues and which may be implemented in AUTO, but we did not use this algorithm here.)

The forced system (1) may also be addressed using the theory and vocabulary of non-autonomous dynamical systems. One is then interested in the *pullback attractor* in the sense given, e.g. by *Kloeden* (2000) and *Langa et al.* (2002). In a nutshell, the pullback attractor at a time t is the set of system solutions compatible with arbitrary initial conditions at time $t - t_b$ as $t_b \to \infty$ [1]. By reasoning on the properties of invariance to time shifts it is easily shown that the pullback attractor at any time is equivalent

[1] The terminology is still debated. *Wiggins* (2003, sect. 8.4) defines a *pullback attracting set* equivalent to the pullback attractor of *Kloeden* (2000) and *Langa et al.* (2002) ; see also *Marín-Rubio and Real* (2009) for further comments.

to the classical attracting set if the system is autonomous. If the system is periodically forced then the pullback attractor at a time t is equivalent to the attracting set of the Poincaré section along the phase of the forcing reached at this time t. It follows that the pullback attractor reduces to a set of points if the system is synchronised on a periodic forcing. The global pullback attractor may then be viewed as a collection of distinct *local* pullback attractors, where the word local is used here in the sense that nearby points are attracted towards this attractor [2]. The cardinality of the global pullback attractor is denoted p. If there is only one possible synchronisation regime as is generally the case, p corresponds to the number of forcing cycles associated with this synchronisation regime ($p = 1$ for 1:1; 2 for 2:1; 3 for 3:2, 3:1, etc.). The demonstration relies again on the system invariance with respect to a time-shift of one forcing period (*Ziperman et al.* (2006) show a very nice illustration of this point). If distinct stable (non-chaotic) synchronisation regimes co-exist, then p should be the sum of the cardinality associated with each synchronisation regime, because all the stable solutions compatible with each synchronisation regime correspond to distinct local pullback attractors. In practice, though, some of these solutions may be very weakly stable and difficult to see.

To illustrate this point the cardinality of the pullback attractor at $t_0 = 0$ is estimated as follows. We establish a uniform grid of 49 initial conditions with $t_I = -t_b$ with t_b large enough for convergence, and count the number of distinct solutions found at t_0. The resulting pattern (Figure 4) is, as expected, equivalent to the bifurcation diagram. For exemple, $p = 3$ in the 3:1 tongue. This method allows one to visualise the 4:3 ($p = 4$) and even the 5:4 ($p = 5$) tongues to the left of the 3:2 tongue. It is also seen that p is generally larger where different synchronisation regimes co-exist. This is the case between the 2:1 and 3:1 regimes around $\gamma = 4$. The signature of the secondary 3:2 synchronisation (in red on Figure 3 within the main 3:2 tongue) is also seen on the full resolution figure (available at `http://www.climate.be/ITOP` (we note, though, the 2:2 and 3:3 solutions mentioned above are too weakly stable for being captured).

3.2 Astronomical forcing

The above non-autonomous framework is naturally suited to address the astronomical forcing. This is the insolation forcing used so far but scaled as follows: $F(t) = (a_{\varepsilon 1})^{-1} \sum a_i \sin(\omega_i + \phi_i)$, were $a_{\varepsilon 1}$ is amplitude of the dominant harmonic associated with obliquity (cf. Figure 1). The purpose of the scaling is simply to make $F(t)$ adimensional.

The cardinality of the global pullback attractor (p) is plotted on Figure 4 (right). Synchronisation occurs

[2] To be precise, *Langa et al.* (2002) only define *local pullback attracting sets*.

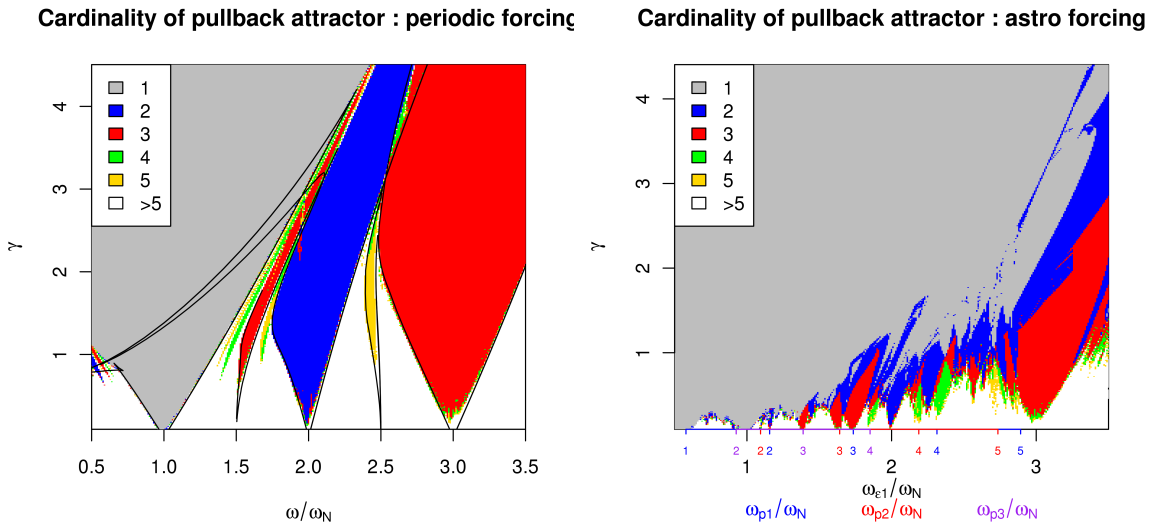

Figure 4: Numerical estimates of the cardinality of the pullback attractor at $t_0 = 0$ for the periodic (left) and astronomically-forced system (right). The cardinality is estimated as the number of different solutions at t_0 considering a grid of 49 initial conditions covering $x \in [-2.2; 2.2]$ and $y \in [-2.2; 2.2]$ at time $t_I = -40T$ for the periodic forcing (T is the period of the forcing), and -1600 ka of real time for the astronomical forcing. Two solutions are estimated to be different if their Euclidean distance is greater than 0.1. The bifurcation diagram of Figure 3 is overlain on the left-hand-side plot to show the equivalence between synchronisation and small cardinality of pullback attractor.

for most parameter configurations. Most frequently, there is one pullback attractor, which corresponds to the strictest definition of the generalised synchronisation regime *Rulkov et al.* (1995). However, there are also parameter sets compatible with $p = 2$, 3 or even more pullback attractors. This is a form of generalised synchronisation where there are different possible stable relationships between the forcing and the response. Three tongues with p=1, 2, 3 are rooted at $\omega/\omega_{\varepsilon 1} = 1$, 2 and 3, respectively, suggesting a synchronisation on the main obliquity component of the astronomical forcing of the same nature as synchronisation on a periodic forcing. A series of other synchronisation tongues with $p > 1$ appear; they correspond to 3:1 ($p = 3$) and 4:1 ($p = 4$) and even 5:1 synchronisation on the three leading components of precession, denoted $p1$, $p2$ and $p3$. Consequently, the richness of the astronomical forcing effectively widens the parameter range for which synchronisation occurs, compared to a periodic forcing. Synchronisations of lower cardinality above these tongues ($p = 1$ or $p = 2$) are then interpreted as a form of combined synchronisation on both obliquity and precession.

It is crucial to appreciate that synchronised solutions are *not* periodic, and unlike the periodic-forcing

case, the different synchronised solutions for a given set of parameters are not time-shifted versions of each other.

In practice, the idea that different synchronised solutions co-exist is of practical relevance for palaeoclimate theory. Namely, the set of parameters used to obtain the fit shown on Figure 2 give two distinct solutions at $t = 0$ when started from a grid of initial conditions at $t_I = -700$ ka. Sensitivity studies show that that the choice of t_b is sometimes important for estimating p. However, tests with t_b as large as $200,000$ ka of astronomical time suggest that several local pullback attractors may co-exist at the asymptotic limit of $t_b = \infty$ for certain parameter sets. This would contradict the conjecture of *Tziperman et al.* (2006).

4 Sensitivity to fluctuations : preliminary results

The stability of a solution to *infinitesimal* perturbations may be measured by the value of the greatest Lyapunov exponent (λ_M) along the solution, averaged over time. Specifically, we consider the greatest Lyapunov exponent characterising the growth of perturbations in the (x,y) phase space. *Pecora and Carroll* (1990) call this the sub-Lyapunov exponent in a similar context. *Wolf et al.* (1985, sect. 3) provide a practical numerical algorithm to estimate the greatest Lyapunov exponent from the differential equations.

Figure 5 shows numerical estimates of λ_M for the periodic-forced system (eq. 1) as a function of γ and ω/ω_N. λ_M is strictly zero for solutions of the autonomous system, as well as for non-synchronised, quasi-periodic solutions. These solutions are indeed neutrally stable against perturbations along the phase direction, and stable against perturbations in the radial direction. λ_M is strictly negative for synchronised solutions, including the suppression regime, because such solutions are stable against fluctuations of the phase *Nicolis* (1987). It follows that $\lambda_M < 0$ may be used as a criteria to detect synchronisation.

In practice, though, we need to quantify to stability of solutions against fluctuations of *finite* amplitude. The normal form of the fold bifurcation help us here to outline a connexion between the greatest Lyapunov exponent (measuring the sensitivity to infinitesimal perturbations) and the probability of a phase-slip (sensitivity to finite perturbations). This normal form is $\dot{x} = x^2 - \mu^2$. The greatest Lyapunov exponent is -2μ on the stable solution. As μ decreases towards zero (equivalent to approaching the edge of the tongue from within the tongue), the stable and unstable solutions are increasingly close to each other. Furthermore, the height of the potential barrier that the stable solution must overcome to leave

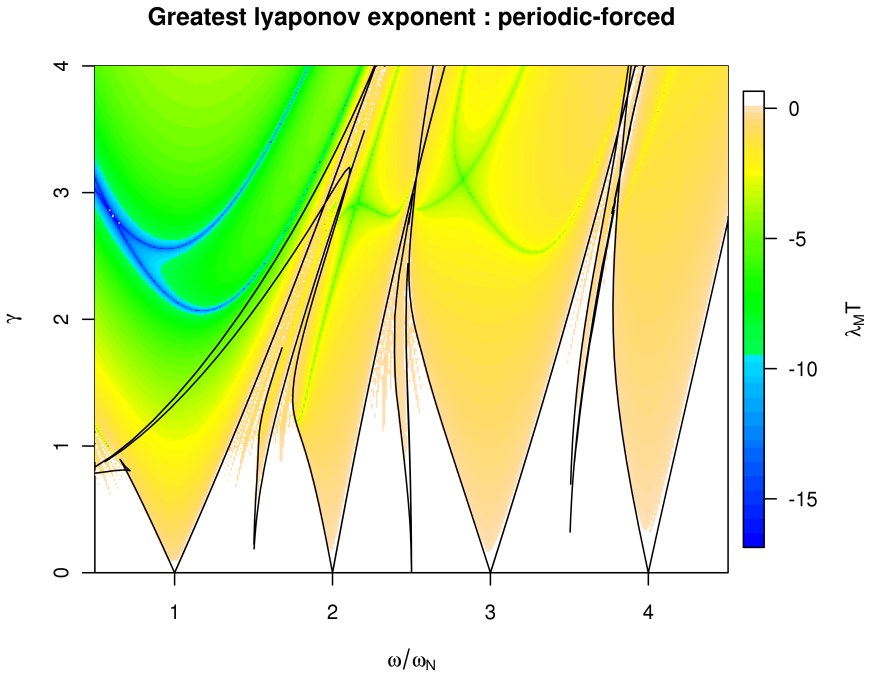

Figure 5: Numerical estimates of the greatest numerical Lyapunov exponent in the periodic-forced system (1). A spin-up procedure starts at $t_I = -150T$ ($T =$ forcing period) in order to find one attractor as well as the direction of the greatest Lyapunov exponent at $t_{I'} = -120T$. The average greatest Lyapunov exponent is then estimated using the procedure described by *Wolf et al.* (1985) over the interval $[t_{I'}; 0]$. The greatest Lyapunov exponent is here expressed by the adimensional number $\lambda_M T$. Bifurcation curves as shown on Figure 3 where overlain in order to highlight the correspondence between negative Lyapunov coefficient and synchronisation.

its basin of attraction is decreased as well. Consequently, the probability of jumping over the boundary of the basin of attraction of the stable solution in response to a *finite* perturbation is increased as one approaches the edge of the tongue. The phenomenon of jumping from one stable phase to another one in response to a fluctuation is called phase slip by *Pikovski et al.* (2001, p. 238).

Consider the astronomical forcing again. To enlighten the discussion we focus on one particular parameter set for which 3 local pullback attractors were found, and we introduce the notion of *basins of attraction* associated to each local pullback attractor at some time t_0. These basins are defined as the sets of initial conditions at t_0 due to converge to the three respective local pullback attractors (*Kloeden* (2000) provides a more formal definition). The basins are plotted on Figure 6, and on this plot are superimposed the sections of the three attractors at t_0—they naturally lie within each of their respective basins

of attraction.

Suppose now that the system is subject to additive fluctuations. The latter may cause a form of phase slip by displacing the trajectory out of its basin of attraction, just as in the periodic forcing case. As a further illustration of this idea we show on Figure 7 two sample trajectories subject to the same system parameters as those used for Figure 2, but with additive fluctuations added to the fast variable (see legend for details). Two phase slips are identified within 800,000 years. A trajectory which follows a local pullback attractor is then expected to be the more stable against fluctuations as it stay away of the limits of the basin of attraction of this attractor.

The hope is that the averaged value of λ_M over this solution is a suitable measure of average stability against finite perturbations, as it is the case with the periodic forcing. We estimated here the average λ_M over a same interval for the three attractors considered on Figure 6. Values for each attractor differ. This suggests that the three attractors are not equally stable and this is a reasonable statement because they are all different. Unfortunately, we found that estimates of the average λ_M depend strongly on the time interval considered for averaging. Robustly ranking the different attractors according to their stability did not prove to be straighforward in this particular case. A complementary article (De Saedeleer et al., to be submitted) focuses on more time-localised measures of stability as well as on the evolving geometry of the basins of attraction.

5 Conclusion

The cardinality of the pullback attractor is a convenient concept to diagnose and understand synchronisation of a system on a quasi-periodic forcing such as the astronomical forcing. Here, we considered a simple palaeoclimate model akin of the Van der Pol oscillator. The relevant feature of this oscillator for palaeoclimate theory is the principle of *relaxation*, in which a fast responding variable (for example, the North Atlantic overturning stream function) is coupled with a slow, time-integrating process, like the growth of ice sheets. One seemingly robust conclusion is that the richness of the astronomical forcing effectively widens the parameter range for which synchronisation occurs compared to a periodic forcing. This is because synchronisation tongues originate at the harmonics of the different components of the forcing. For low forcing amplitude the regime within these tongues is similar to a response to a periodic forcing. As this amplitude is increased the different components of the forcing (precession and obliquity) interact and the number of possible synchronised solutions is reduced. It is therefore conceivable that the climate system wandered throughout preferential synchronisation regimes on obliquity, precession,

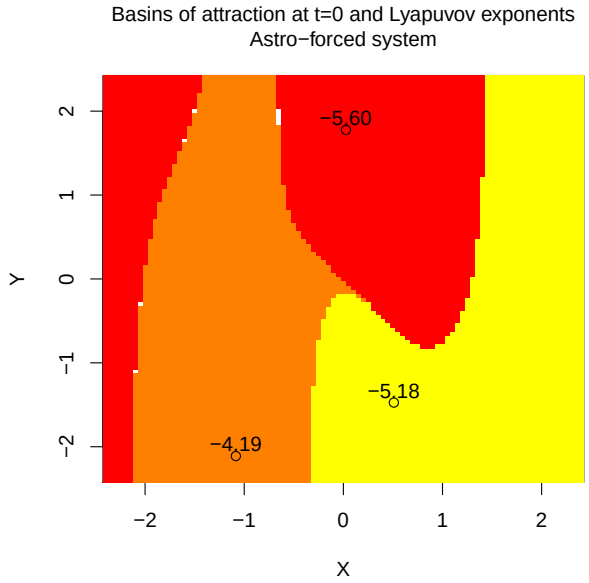

Figure 6: Basins of attractions for astronomically-forced system at time $t_0 = 0$ estimated as follows. Three pullback attractors are identified at t_0 based on a grid of initial conditions at t_I=-1600 ka of astronomical time. The attractors at $t_0 = 0$ are represented as dots in the x, y phase space. Color shades represent the three sets of initial conditions at t_0 due to converge to the three pullback attractors in the future (in practice we waited until $t_1 = +1600$ ka to attribute each initial condition to a given attractor). Numbers are the greatest Lyapunov exponents expressed in the adimensional form $\lambda_M 2\pi/\omega_{\varepsilon 1}$, averaged along the three pullback attractors over the time $[t_0; t_1]$. Note that this measure differs for each attractor, but it is also sensitive to the exact time interval considered for averaging. We used $\alpha = 11.1$, $\beta = 0.25$, $\gamma = 0.5$ and $\tau = 42\,ka$, corresponding to $\omega_{\varepsilon 1} = 2.92\omega_N$.

or combinations of both, as environmental parameters varied throughout the history of the Pleistocene. The second conclusion is related: as long as the forcing is not too large different synchronised solutions may co-exist and moderate fluctuations may effectively induce jumps between these different solutions, equivalent to phase slips described for periodic forcing. These jumps effectively restrict the prediction horizon of the exact course of climate evolution at theses time scales.

Throughout this study appeared a tension between the theory—concepts and theorems are valid at the asymptotic limit t or $t_b \to \infty$—and the practical needs of palaeoclimate theory. Indeed, it does not make much sense to consider prediction horizons much beyond 1,000 ka in this context because the system can no longer be assumed to be stationary. For this reason, we encourage to continue the development of more time-local concepts, for example 'episodic' synchronisation.

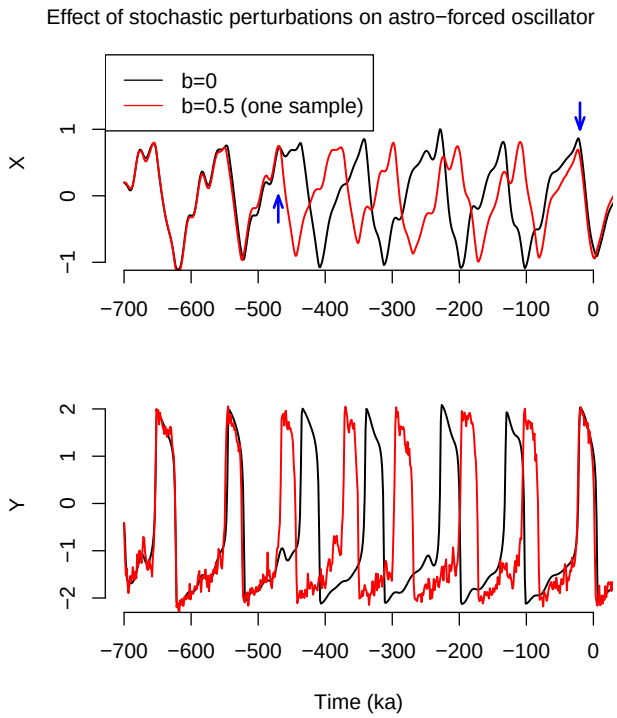

Figure 7: The solution of eq. (1) as in Figure 2 is plotted (black) along with one sample trajectory of the same system (red), but with $\mathrm{d}y = -\tau a^{-1}(\alpha(\psi'(y) - x))\mathrm{d}t + b\mathrm{d}\omega$, with $b = 0.5/\sqrt{\omega_{\varepsilon 1}}$ and ω a Wiener-process. Arrows show the times of the two phase slips.

Note on parameters

The reader may have noted that different parameter sets where used to produce Figures 2 and 7 than for the other figures. $\alpha = 30$ and $\beta = 0.75$ indeed give the best fit to data, but the system is then very stiff and exploring its bifurcation structure requires algorithms specifically designed for slow-fast systems (e.g. *Desroches et al.*, 2010) that fall beyond the focus of the present contribution. The main conclusions are generally unchanged, but it was seen that regimes for which different pullback attractors co-exist under astronomical forcing are less frequent when β is increased. The increase in α has little impact. The reader is encouraged to produce further diagrams using the source code available at `http://www.climate.be/ITOP`..

Acknowledgments

Sebastian Wieczorek (University of Exeter) provided guidance for the calculation of greatest Lyapunov exponent and calculation of bifurcation diagrams. James Robinson (Univerisity of Warwick) provided useful references to pullback attractor theory. M. Ghil (ENS, Paris) draw our attention on the similarity between Saltzman's model and the Van der Pol oscillator. The project is funded by the ERC-starting grant 'Integrated Theory and Observations of the Pleistocene'; MC is research associate with the Belgian National Fund of Scientific Research. The article was written when MC visited the Isaac Newton Institute in Cambridge. Figures and calculations where made with the R language and the Intel Fortran Compiler.

References

Balanov, A., N. Janson, D. Postnov, and O. Sosnovtseva, *Synchronization : from simple to complex*, Springer Series in Synergetics, Springer, 2009.

Benzi, R., G. Parisi, A. Sutera, and A. Vulpiani, Stochastic resonance in climatic change, *Tellus*, *34*(1), 10–16, 1982.

Berger, A. L., Long-term variations of daily insolation and Quaternary climatic changes, *J. Atmos. Sci.*, *35*, 2362–2367, 1978.

Desroches, M., B. Krauskopf, and H. M. Osinga, Numerical continuation of canard orbits in slow-fast dynamical systems, *Nonlinearity*, *23*(3), 2010.

Dijkstra, H. A., and W. Weijer, Stability of the global ocean circulation: Basic bifurcation diagrams, *Journal of Physical Oceanography*, *35*(6), 933–948, doi:10.1175/JPO2726.1, 2005.

Doedel, E. J., and B. E. Oldeman, AUTO-07P: continuation and bifurcation software for ordinary differential equations, *Tech. rep.*, Concordia University, Montreal, Canada, 2009.

Ghil, M., and H. Le Treut, A climate model with cryodynamics and geodynamics, *J. Geophys. Res.*, *86*(C6), 5262–5270, 1981.

Grassberger, P., Do climatic attractors exist?, *Nature*, *323*(6089), 609–612, 1986.

Grassberger, P., and I. Procaccia, Characterization of strange attractors, *Physical Review Letters*, *50*(5), 346–349, 1983.

Guckenheimer, J., and P. Holmes, *Nonlinear Oscillations, Dynamical Systems, and Bifurcations of Vector Fields*, no. 42 in Applied Mathematical Sciences, Springer-Verlag, New York, NY, 1983.

Hays, J. D., J. Imbrie, and N. J. Shackleton, Variations in the Earth's orbit : Pacemaker of ice ages, *Science*, *194*, 1121–1132, 1976.

Huybers, P., Glacial variability over the last two millions years: an extended depth-derived age model, continous obliquity pacing, and the Pleistocene progression, *Quaternary Sci. Rev.*, *26*, 37–55, doi: 10.1016/j.quascirev.2006.07.013, 2007.

Kloeden, P. E., A Lyapunov function for pullback attractor of nonautonomous differential equations, *Electro. J. Diff. Eqns, Conf.*, *5*, 91–102, 2000.

Langa, J. A., J. C. Robinson, and A. Suárez, Stability, instability, and bifurcation phenomena in non-autonomous differential equations, *Nonlinearity*, *15*(3), 887, 2002.

Laskar, J., P. Robutel, F. Joutel, F. Boudin, M. Gastineau, A. C. M. Correia, and B. Levrard, A long-term numerical solution for the insolation quantities of the Earth, *Astron. Astroph.*, *428*, 261–285, 2004.

Lisiecki, L. E., and M. E. Raymo, A Pliocene-Pleistocene stack of 57 globally distributed benthic δ^{18}O records, *Paleoceanogr.*, *20*, PA1003, doi:10.1029/2004PA001071, 2005.

Lisiecki, L. E., and M. E. Raymo, Plio-Pleistocene climate evolution: trends and transitions in glacial cycles dynamics, *Quaternary Sci. Rev.*, *26*, 56–69, doi:10.1016/j.quascirev.2006.09.005, 2007.

Marín-Rubio, P., and J. Real, On the relation between two different concepts of pullback attractors for non-autonomous dynamical systems, *Nonlinear Analysis: Theory, Methods and Applications*, *71*(9), 3956 – 3963, doi:DOI: 10.1016/j.na.2009.02.065, 2009.

Mettin, R., U. Parlitz, and W. Lauteborn, Bifurcation structure of the driven van der pol oscillator, *International Journal of Bifurcation and Chaos*, *3*(6), 1529–1555, doi:10.1142/S0218127493001203, 1993.

Milankovitch, M., *Canon of insolation and the ice-age problem*, Narodna biblioteka Srbije, Beograd, english translation of the original 1941 publication, 1998.

Mudelsee, M., and K. Stattegger, Application of the grassberger-. procaccia algorithm to the 6180 record from odp site 659: selected methodical aspects, in *Fractals and dynamics systems in geosciences*, edited by J. H. Kruhl, pp. 399–413, Springer-Verlag, 1994.

Nicolis, C., Stochastic aspects of climatic transitions — response to a periodic forcing, *Tellus*, *34*(1), 1–9, 1982.

Nicolis, C., Climate predictability and dynamical systems, in *Irreversible phenomena and dynamical system analysis in the geosciences*, *NATO ASI series C : Mathematical and Physical Sciences*, vol. 192, edited by C. Nicolis and G. Nicolis, pp. 321–354, Kluwer, 1987.

Nicolis, C., and G. Nicolis, Stochastic aspects of climatic transitions — additive fluctuations, *Tellus*, *33*(3), 225–234, 1981.

Nicolis, C., and G. Nicolis, Is there a climatic attractor?, *Nature*, *311*(5986), 529–532, 1984.

Nicolis, C., and G. Nicolis, Reconstruction of the dynamics of the climatic system from time-series data, *Proc. Natl. Acad. Sci. USA*, *83*(536-540), 1986.

Paillard, D., and F. Parrenin, The Antarctic ice sheet and the triggering of deglaciations, *Earth Planet. Sc. Lett.*, *227*, 263–271, 2004.

Pecora, L. M., and T. L. Carroll, Synchronization in chaotic systems, *Phys. Rev. Lett.*, *64*(8), 821–824, doi:10.1103/PhysRevLett.64.821, 1990.

Petit, J. R., et al., Climate and atmospheric history of the past 420, 000 years from the Vostok ice core, Antarctica, *Nature*, *399*, 429–436, 1999.

Pikovski, A., M. Rosenblum, and J. Kurths, *Synchronization: a universal concept in nonlinear sciences*, *Cambridge Nonlinear Science Series*, vol. 12, Camb. Univ. Press, 2001.

Rahmstorf, S., et al., Thermohaline circulation hysteresis: A model intercomparison, *Geophys. Res. Lett.*, *32*(23), L23,605, 2005.

Rulkov, N. F., M. M. Sushchik, L. S. Tsimring, and H. D. I. Abarbanel, Generalized synchronization of chaos in directionally coupled chaotic systems, *Phys. Rev. E*, *51*(2), 980–994, doi:10.1103/PhysRevE.51.980, 1995.

Saltzman, B., A. R. Hansen, and K. A. Maasch, The late Quaternary glaciations as the response of a 3-component feedback-system to Earth-orbital forcing, *Journal of the Atmospheric Sciences*, *41*(23), 3380–3389, 1984.

Schilder, F., and B. B. Peckham, Computing arnol'd tongue scenarios, *J. Comput. Phys.*, *220*(2), 932–951, doi:http://dx.doi.org/10.1016/j.jcp.2006.05.041, 2007.

Tziperman, E., and H. Gildor, On the mid-Pleistocene transtion to 100-kyr glacial cycles and the asymmetry between glaciation and deglaciation times, *Paleoceanography*, *18*(1), 1001, doi:10.1029/2001PA00027, 2003.

Tziperman, E., M. E. Raymo, P. Huybers, and C. Wunsch, Consequences of pacing the Pleistocene 100 kyr ice ages by nonlinear phase locking to Milankovitch forcing, *Paleoceanography*, *21*, PA4206, doi:10.1029/2005PA001241, 2006.

Vautard, R., and M. Ghil, Singular spectrum analysis in nonlinear dynamics, with applications to paleoclimatic time-series, *Physica D*, *35*(3), 395–424, 1989.

Wiggins, S., *Introduction to Applied Nonlinear Dynamical Systems and Chaos*, 2nd ed., Springer, 2003.

Wolf, A., J. B. Swift, H. L. Swinney, and J. A. Vastano, Determining lyapunov exponents from a time series, *Physica D: Nonlinear Phenomena*, *16*(3), 285–317, 1985.